

# SPECULAR MULTIPATH EXPLOITATION FOR IMPROVED VELOCITY ESTIMATION IN THROUGH-THE-WALL RADAR IMAGING

Michael Leigsnering\*    Fauzia Ahmad†    Moeness G. Amin†    Abdelhak M. Zoubir\*

\*Signal Processing Group, Institute of Telecommunications  
Technische Universität Darmstadt, 64283 Darmstadt, Germany

†Radar Imaging Laboratory, Center for Advanced Communications  
Villanova University, Villanova, PA 19085 USA

## ABSTRACT

Through-the-wall radar imaging aims at determining the locations and velocities of obscured targets. The slow velocities of indoor targets are in particular difficult to detect and estimate. It is shown by theoretical considerations and simulation that indirect propagation paths contain significant information on the target movements, which can be utilized for improved sensing. We propose a compressive sensing based method that exploits a multipath model to improve the velocity resolution of the reconstruction. Simulation results demonstrate the effectiveness of the proposed approach.

**Index Terms**— Through-the-wall, radar imaging, multipath exploitation, compressive sensing

## 1. INTRODUCTION

Through-the-wall radar imaging (TWRI) has gained attention due to its ability to acquire accurate information of scenes behind walls or other opaque obstacles utilizing electromagnetic (EM) wave propagation [1–5].

In many scenarios, it is desirable to obtain information on both the location and velocity of the targets. High-resolution images require large apertures and signal bandwidths, translating into large amounts of data. Resolving the low velocities of indoor targets may pose an even harder challenge. In particular, movements parallel to the array (i.e. in the crossrange direction) cause zero Doppler shift and, as such, are difficult to detect. Multipath propagation is considered a nuisance if it cannot be traced back to the target producing it. On the other hand, if target-multipath association is possible, additional information on the target velocity can be obtained from the multipath returns. We propose a multipath exploitation scheme that improves crossrange velocity resolution.

Earlier work focused on mitigating the effects of multipath propagation in TWRI [6]. Later, multipath exploitation

was examined to improve the performance of the imaging system. Extending the imaged region [7] or reducing multipath ghosts while increasing the signal-to-clutter ratio [8] has been the next step of research. In order to tackle the huge amount of data to be acquired and processed, the application of compressive sensing (CS) has been proposed for TWRI. After the first attempt in [9], others utilize subsequently CS to obtain high quality images [10–12]. Reconstruction of stationary and moving targets [12] as well as multipath exploitation of stationary targets [13, 14] have been investigated in the context of CS.

In this paper, we consider both stationary and moving targets and aim at exploiting multipath in order to improve the velocity resolution in the reconstructed scene. A specular multipath model, developed by the authors in [13], is generalized to include the response of moving targets. The model is used in a group sparse CS reconstruction to fully utilize the velocity information contained in the indirect propagation paths. We present simulation results that illustrate the superior velocity resolution when exploiting multipath.

The remainder of the paper is organized as follows. The signal model for pulsed radar operation in multipath environments is introduced in Section 2. In Section 3, we describe the proposed CS based reconstruction approach, followed by a discussion on the concept of apparent Doppler velocity in Section 4. Supporting simulation results are presented in Section 5. We draw conclusions in Section 6.

## 2. SIGNAL MODEL

In this section, we describe the signal model for an ultra-wideband multistatic radar system with a single transmitter and  $N$  receivers. The model extends that of [12] to include target multipath from interior walls.

We assume  $P$  point targets, each undergoing a translatory or linear motion with constant velocity in a 2D space. We consider a coherent processing interval (CPI) of  $K$  wide-band pulses and a pulse repetition interval (PRI) of  $T_r$ . The pulse index  $k = 0, \dots, K - 1$  is referred to as slow time.

The work by F. Ahmad and M. Amin was supported by ARO and ARL under contract W911NF-11-1-0536.

Hence, if the PRI is sufficiently small, movement of indoor targets should be approximately of constant velocity and slow enough so that targets do not move out of a range cell. Note that stationary targets are also included in this model and correspond to zero velocity. Using these assumptions, we establish that the  $p$ th target at pulse  $k$  is located at position

$$\mathbf{x}_p(k) = (x_p + v_{xp}kT_r, y_p + v_{yp}kT_r), \quad (1)$$

where  $(x_p, y_p)$  is the position of the  $p$ th target at  $t = 0$  and  $(v_{xp}, v_{yp})$  is the corresponding velocity vector.

The emitted pulses are wideband with duration  $\tilde{T}$  and can be expressed as  $\Re\{s(t) \exp(j2\pi f_c t)\}$ , where  $t$  is the fast time,  $s(t)$  is the pulse in the complex baseband, and  $f_c$  is the carrier frequency. The pulses travel through the exterior wall to the  $P$  point targets and are reflected back to the receive array. The radar return measured by the  $n$ th receiver corresponding to the  $k$ th pulse is given by

$$z_{nk}(t) = \sum_{p=0}^{P-1} \sigma_p s(t - kT_r - \tau_{pn}(k)) \times \exp(-j2\pi f_c (kT_r + \tau_{pn}(k))) \quad (2)$$

where  $\sigma_p$  is the complex reflectivity of the  $p$ th point target and  $\tau_{pn}(k)$  is the bistatic propagation delay from the transmitter to the  $p$ th target and back to the  $n$ th receiver. Note that the delays and the received signal generally depend on the slow time index  $k$ . However, if the  $p$ th target has zero velocity, as in the stationary case, the delays do not change with  $k$ .

The discrete model is generated by sampling the targets' locations and velocities at  $N_p$  and  $N_v$  points, respectively. Each grid point assumes a certain reflectivity, whereas a non-existing target can be represented by zero reflectivity. Hence, in total, we have  $N_p N_v$  possible target states, which can be stacked into an  $N_p N_v \times 1$  vector  $\boldsymbol{\sigma}$ . The received signal  $z_{nk}(t)$  is sampled uniformly at  $T$  time steps with sampling interval  $T_s$ . The sampling interval should be chosen to attain the Nyquist rate of the wideband pulse  $s(t)$ . The samples can be stacked into a  $T \times 1$  vector  $\mathbf{z}_{nk}$  defined as

$$\mathbf{z}_{nk} = \boldsymbol{\Psi}_{nk} \boldsymbol{\sigma}, \quad (3)$$

where  $\boldsymbol{\Psi}_{nk}$  are the dictionary matrices, which can be obtained by discretizing the right hand side of (2).

Stacking all of the received signal vectors  $\{\mathbf{z}_{nk}, n = 0, \dots, N-1, k = 0, \dots, K-1\}$  results in a  $TNK \times 1$  measurement vector  $\mathbf{z}$  and a  $TNK \times N_p N_v$  dictionary matrix  $\boldsymbol{\Psi}$ . Hence, we obtain

$$\mathbf{z} = \boldsymbol{\Psi} \boldsymbol{\sigma}. \quad (4)$$

The above equation represents the linear model for the direct returns of the wideband pulsed radar. However, so far, multipath propagation has not been taken into account, which is treated in the following subsection.

## 2.1. Multipath Returns

In a multipath environment, the transmitted pulse may reach the receiver via an additional reflection at a secondary scatterer (usually an interior wall). The two-way propagation delays can be calculated through geometrical optics principles for direct and multipath propagation [13]. The receiver adds the returns from all possible propagation paths  $r = 0, \dots, R-1$ , yielding

$$\mathbf{z} = \boldsymbol{\Psi}^{(0)} \boldsymbol{\sigma}^{(0)} + \boldsymbol{\Psi}^{(1)} \boldsymbol{\sigma}^{(1)} + \dots + \boldsymbol{\Psi}^{(R-1)} \boldsymbol{\sigma}^{(R-1)}. \quad (5)$$

Note that  $r = 0$  corresponds to the direct path and the remaining  $R-1$  are the multipaths. The dictionaries  $\boldsymbol{\Psi}^{(r)}$ ,  $r = 1, 2, \dots, R-1$  are defined as in the direct propagation case except that the two-way delays are calculated for the  $r$ th propagation path. We assume an individual target state vector  $\boldsymbol{\sigma}^{(r)}$  for each path. This is because the phase and amplitude of the target reflectivity, in general, change with the bistatic and aspect angles. For notational convenience, path losses have been absorbed into the corresponding target state vectors. Further note that we assume the same number of propagation paths for each target in (5). This can be done without loss of generality, as the reflectivity can be set to zero if the corresponding path is not available for a particular target.

## 3. GROUP SPARSE SCENE RECONSTRUCTION

Next, we obtain the complete target information, i.e., location and velocity, using CS principles. A high-dimensional model is constructed using (5) in order to account for all propagation paths. Since we aim at obtaining a faithful reconstruction using a reduced set of measurements in (5), the corresponding signal model can be expressed as,

$$\bar{\mathbf{z}} = \boldsymbol{\Phi} \tilde{\boldsymbol{\Psi}} \tilde{\boldsymbol{\sigma}}, \quad (6)$$

where  $\tilde{\boldsymbol{\Psi}} = [\boldsymbol{\Psi}^{(0)} \boldsymbol{\Psi}^{(1)} \dots \boldsymbol{\Psi}^{(R-1)}] \in \mathbb{C}^{TNK \times N_p N_v R}$  is the concatenated overcomplete dictionary for all possible paths and  $\boldsymbol{\Phi}$  is a suitable downsampling operation as described in [12]. The unknown target reflectivity vectors are stacked to form one tall vector

$$\tilde{\boldsymbol{\sigma}} = \left[ \left( \boldsymbol{\sigma}^{(0)} \right)^T \left( \boldsymbol{\sigma}^{(1)} \right)^T \dots \left( \boldsymbol{\sigma}^{(R-1)} \right)^T \right]^T \in \mathbb{C}^{N_p N_v R}. \quad (7)$$

Given the reduced measurements  $\bar{\mathbf{z}}$  in (6), we aim at recovering the target state information  $\tilde{\boldsymbol{\sigma}}$  using CS reconstruction. Similar to [13], we exploit multipath by utilizing the group sparse structure in the target state information. The state vectors  $\boldsymbol{\sigma}^{(r)}$ , corresponding to the  $R$  paths, exhibit a group sparse structure, where the individual groups extend across the paths for each target state. Note that the apparent Doppler speed for a particular target may differ when observed through different paths. This, however, is incorporated in the model, as delays  $\tau_{pn}^{(r)}(k)$  depend on the slow time and

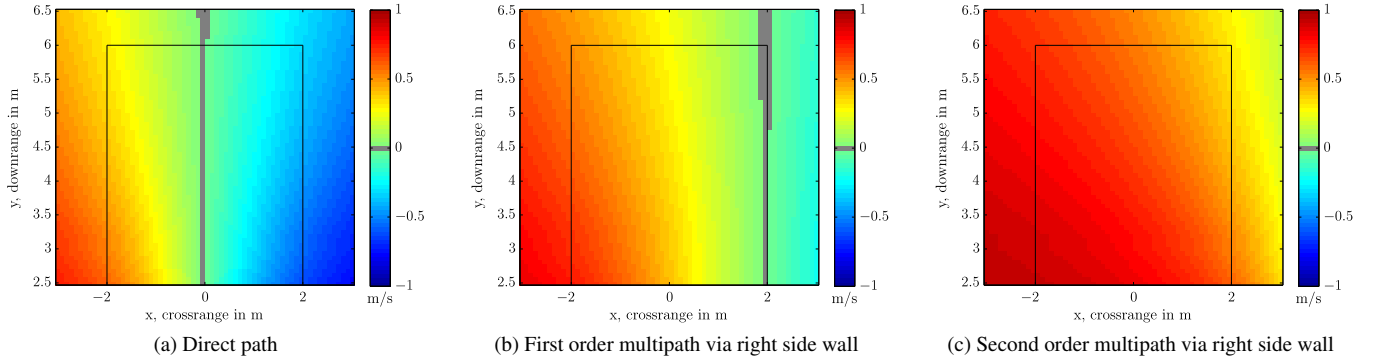


**Fig. 1.** Apparent Doppler velocity for a target moving with velocity  $(1, 0)$  m/s.

are all calculated based on the same coordinate system. In this way, the reconstruction benefits from additional diversity in the received signal due to different Doppler shifts from the same target.

Employing a group sparse reconstruction approach results in the optimization problem

$$\hat{\sigma} = \arg \min_{\tilde{\sigma}} \|\tilde{z} - \Phi \tilde{\Psi} \tilde{\sigma}\|_2^2 + \lambda \|\tilde{\sigma}\|_{1,2}, \quad (8)$$

where

$$\|\tilde{\sigma}\|_{1,2} = \sum_{p=0}^{N_p N_w - 1} \left\| \left[ \sigma_p^{(0)}, \sigma_p^{(1)}, \dots, \sigma_p^{(R-1)} \right]^T \right\|_2 \quad (9)$$

and  $\lambda$  is a regularization parameter. (8) can be solved using SparSA [15] or other available schemes [16, 17].

Once a solution  $\hat{\sigma}$  is obtained, the individual target state vectors can be combined non-coherently to form a composite target state vector. The final recovery result contains the information of the location and the translatory motion of all targets. For an in-depth treatment of the group-sparse reconstruction approach, refer to [13].

#### 4. APPARENT DOPPLER VELOCITY

In order to motivate the exploitation of multipath, we examine the information contained in the multipath returns. A target at position  $(x_p, y_p)$  moving with velocity  $(v_{xp}, v_{yp})$  has an apparent Doppler velocity  $v_D$ . In the case of direct propagation, this is simply the radial velocity component with respect to the center of the array. However, if the wave travels on an indirect path, this apparent Doppler velocity changes. The multipath can be cast as direct propagation to a virtual array, whose element locations are dictated by the physical array and the secondary scatterers (interior walls). As such, for apparent Doppler velocity corresponding to multipath propagation, the radial velocity component with respect to the center of the corresponding virtual array is a relevant measure. The apparent Doppler velocity may also be approximated using the propagation delays. Depending on the receiver  $n$ , the path  $r$ , and averaging over the full CPI, the apparent Doppler ve-

locity for the  $p$ th target may be expressed as

$$v_{D,pn}^{(r)} = \frac{1}{K-1} \sum_{k=0}^{K-2} c \frac{\tau_{pn}^{(r)}(k+1) - \tau_{pn}^{(r)}(k)}{T_r}. \quad (10)$$

For illustration, we simulate a target at an arbitrary location within three walls, moving with a velocity  $(v_{xp}, v_{yp}) = (1, 0)$  m/s. Hence, the target is solely moving in the crossrange direction and the apparent Doppler velocity is zero in the broadside direction of the array. At each assumed target position, the apparent Doppler velocity is color coded in Fig. 1. The surrounding walls are also superimposed on the figure. In the direct propagation case, shown in Fig. 1a, we observe the expected pattern, with zero velocity along broadside and gradually increasing velocity for angles deviating from broadside. However, the pattern is different for an indirect path, reaching the target via reflection at the right side wall, as shown in Figs. 1b,c. Fig. 1b corresponds to a first order multipath that involves direct propagation on transmit and a secondary reflection at the right side wall on receive, whereas Fig. 1c involves a secondary reflection at the right side wall on both transmit and receive. The patterns in Figs. 1b, c are shifted and distorted as compared to Fig. 1a. In particular, the zero velocity line is shifted as compared to that in Fig. 1a. Hence, we obtain additional information on target motion through the first and second order multipath returns. If properly modeled, as described earlier, this property is exploited to improve the velocity estimation.

#### 5. SIMULATION RESULTS

Simulations were performed for a wideband real aperture pulse-Doppler radar with one transmitter and a uniform linear array with  $N = 11$  receivers. A modulated Gaussian pulse, centered at  $f_c = 2$  GHz, with a relative bandwidth of 50% is transmitted. The PRI is set to 10 ms and  $K = 15$  pulses are coherently processed. At the receive side,  $T = 150$  fast time samples in the relevant interval, covering the target and multipath returns, are taken at a sampling rate of 4 GHz. The receive array with 10 cm interelement spacing is centered

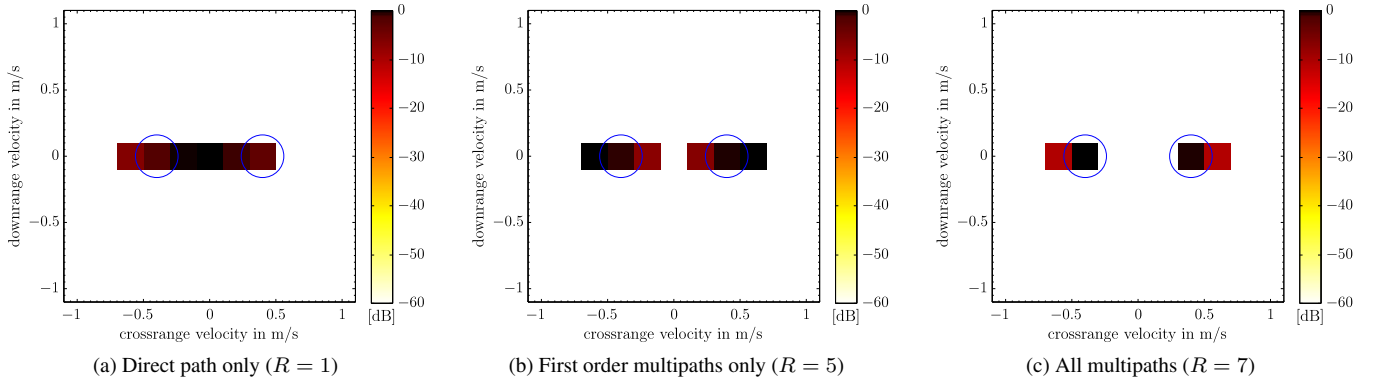


Fig. 2. CS reconstruction results for various amounts of multipath.

around the transmitter and is located parallel to the exterior front wall at 3 m distance. The front wall is modeled with 20 cm thickness and relative permittivity of 7.66. Two side walls are considered at  $\pm 2$  m that cause 3 different multipaths each. There are in total 4 first order multipaths and 2 second order multipaths, i.e.,  $R = 7$  paths are considered in the received signal. We do not consider any front wall returns as they can be removed by time-gating [12] or using other wall mitigation techniques [18–20]. As we intend to focus on velocity estimation, we keep the target(s) fixed at 4 m downrange in the broadside direction of the receive array.

First, we show that the additional information on the target velocity contained in the multipath returns can be exploited to improve the velocity resolution. We employ the proposed CS reconstruction scheme to resolve two targets with similar velocities. Both targets reside in the same range/crossrange cell, but move in opposing crossrange directions. The velocities differ by only 0.8 m/s. Further, we reduce the number of measurements to one-half of the receive elements and one-third of the fast time samples. We show the results for different numbers of multipath: the direct propagation path only, five propagation paths (first order multipath returns only) and all seven paths as described above. As evident from Fig. 2, the velocity resolution capabilities improve with incorporation of an increasing number of multipath returns. If only the direct path is available, the two moving targets cannot be resolved. If the four first order multipath returns are included and exploited, the two targets are resolved, but the velocity estimates are biased. Finally, if all seven paths are available and exploited, the two moving targets are resolved with accurate velocity estimates.

Further, we quantify the resolution performance for various number of multipaths. We use the same setup as in the previous example. However, we change the velocity difference from 0.4 m/s to 2 m/s in steps of 0.4 m/s. We also consider the total number of paths,  $R$ , to be one, five, six, and seven, i.e. direct path only, first order multipaths only, and one or both second order multipaths. We repeat the experiment 100 times and use a simplistic detection scheme to get

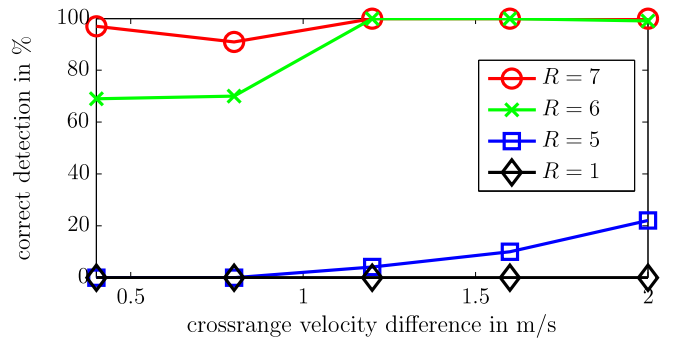


Fig. 3. Crossrange resolution performance for various amounts of multipath.

an upper bound on the performance. More specifically, we take the two strongest pixels and check if they correspond to the true target velocities. While in real life this detection scheme is not feasible, it serves as a suitable metric to provide a fair comparison for the examined cases. The results are depicted in Fig. 3. It can be seen that without multipath, the two velocities cannot be resolved at all. For increasing number of multipath returns, the resolution capabilities improve. For  $R = 7$ , we can (almost) perfectly resolve even the smallest velocity difference. As evident from the above results, it is advantageous to exploit the information contained in the multipath returns for improved scene reconstruction.

## 6. CONCLUSION

Based on a multipath propagation and motion model for indoor targets in TWRI, we proposed a CS based reconstruction approach that exploits target-wall multipath to improve target velocity estimation. The model does not require resolvable multipaths and, as such avoids the need for associating radar returns with the interior reflecting walls. Simulations demonstrated the merits of multipath exploitation in enhancing imaging resolution, which generally benefits from an increased number of multipath returns that may encompass first and second order types of reflections.

## 7. REFERENCES

- [1] M.G. Amin and F. Ahmad, "Through-the-wall radar imaging: Theory and applications," in *E-reference Signal Processing*, R. Chellappa and S. Theodoridis, Eds., vol. 2. Elsevier, 2013.
- [2] E.J. Baranoski, "Through-wall imaging: Historical perspective and future directions," *Journal of the Franklin Institute*, vol. 345, no. 6, pp. 556 – 569, Sep. 2008.
- [3] M.G. Amin, Ed., *Through-the-Wall Radar Imaging*, CRC Press, 2011.
- [4] M.G. Amin and F. Ahmad, "Wideband synthetic aperture beamforming for through-the-wall imaging [lecture notes]," *IEEE Signal Processing Magazine*, vol. 25, no. 4, pp. 110 –113, July 2008.
- [5] H. Burchett, "Advances in through wall radar for search, rescue, and security applications," in *IET Conf. on Crime and Security*, June 2006, pp. 511–525.
- [6] F. Ahmad and M.G. Amin, "Multi-location wideband synthetic aperture imaging for urban sensing applications," *Journal of the Franklin Institute*, vol. 345, no. 6, pp. 618 – 639, Sep. 2008.
- [7] S. Kidera, T. Sakamoto, and T. Sato, "Extended imaging algorithm based on aperture synthesis with double-scattered waves for UWB radars," *IEEE Transactions on Geoscience and Remote Sensing*, vol. 49, no. 12, pp. 5128 – 5139, Dec. 2011.
- [8] P. Setlur, M. Amin, and F. Ahmad, "Multipath model and exploitation in through-the-wall and urban radar sensing," *IEEE Transactions on Geoscience and Remote Sensing*, vol. 49, no. 10, pp. 4021–4034, Oct. 2011.
- [9] Y.-S. Yoon and M.G. Amin, "Compressed sensing technique for high-resolution radar imaging," in *Proceedings of SPIE Signal Processing, Sensor Fusion, and Target Recognition XVII*, Orlando, USA, March 2008, vol. 6968, p. 69681A.
- [10] Q. Huang, L. Qu, B. Wu, and G. Fang, "UWB through-wall imaging based on compressive sensing," *IEEE Transactions on Geoscience and Remote Sensing*, vol. 48, no. 3, pp. 1408 –1415, 2010.
- [11] M. Leigsnering, C. Debes, and A.M. Zoubir, "Compressive sensing in through-the-wall radar imaging," in *IEEE International Conference on Acoustics, Speech and Signal Processing (ICASSP)*, Prague, Czech Republic, May 2011.
- [12] J. Qian, F. Ahmad, and M. G. Amin, "Joint localization of stationary and moving targets behind walls using sparse scene recovery," *Journal of Electronic Imaging*, vol. 22, no. 2, pp. 021002, June 2013.
- [13] M. Leigsnering, F. Ahmad, M.G. Amin, and A.M. Zoubir, "Multipath exploitation in through-the-wall radar imaging using sparse reconstruction," *IEEE Transactions on Aerospace and Electronic Systems*, 2013, In press.
- [14] G. Gennarelli, I. Catapano, and F. Soldovieri, "RF/microwave imaging of sparse targets in urban areas," *IEEE Antennas Wireless Propag. Lett.*, vol. 12, pp. 643–646, May 2013.
- [15] S.J. Wright, R.D. Nowak, and M.A.T. Figueiredo, "Sparse reconstruction by separable approximation," *IEEE Transactions on Signal Processing*, vol. 57, no. 7, pp. 2479–2493, July 2009.
- [16] Y.C. Eldar, P. Kuppinger, and H. Bolcskei, "Block-sparse signals: Uncertainty relations and efficient recovery," *IEEE Transactions on Signal Processing*, vol. 58, no. 6, pp. 3042 –3054, June 2010.
- [17] R.G. Baraniuk, V. Cevher, M.F. Duarte, and Chinmay Hegde, "Model-based compressive sensing," *IEEE Transactions on Information Theory*, vol. 56, pp. 1982–2001, April 2010.
- [18] M. Dehmollaian and K. Sarabandi, "Refocusing through building walls using synthetic aperture radar," *IEEE Transactions on Geoscience and Remote Sensing*, vol. 46, no. 6, pp. 1589–1599, 2008.
- [19] F. H. C. Tivive, A. Bouzerdoum, and M. G. Amin, "An SVD-based approach for mitigating wall reflections in through-the-wall radar imaging," in *IEEE Radar Conference (RADAR)*, Kansas City, USA, May 2011, pp. 519–524.
- [20] Y.-S. Yoon and M.G. Amin, "Spatial filtering for wall-clutter mitigation in through-the-wall radar imaging," *IEEE Transactions on Geoscience and Remote Sensing*, vol. 47, no. 9, pp. 3192 –3208, Sept. 2009.